Critical and Strong-Coupling Phases in One- and Two-Bath Spin-Boson Models

Cheng Guo,[1] Andreas Weichselbaum,[1] Jan von Delft,[1] and Matthias Vojta[2]
[1]Ludwig-Maximilians-Universität München, 80333 Munich, Germany
[2]Institut für Theoretische Physik, Technische Universität Dresden, 01062 Dresden, Germany
(Received 11 November 2011; published 18 April 2012)

For phase transitions in dissipative quantum impurity models, the existence of a quantum-to-classical correspondence has been discussed extensively. We introduce a variational matrix product state approach involving an optimized boson basis, rendering possible high-accuracy numerical studies across the entire phase diagram. For the sub-Ohmic spin-boson model with a power-law bath spectrum $\propto \omega^s$, we confirm classical mean-field behavior for $s < 1/2$, correcting earlier numerical renormalization-group results. We also provide the first results for an XY-symmetric model of a spin coupled to two competing bosonic baths, where we find a rich phase diagram, including both critical and strong-coupling phases for $s < 1$, different from that of classical spin chains. This illustrates that symmetries are decisive for whether or not a quantum-to-classical correspondence exists.

DOI: 10.1103/PhysRevLett.108.160401 PACS numbers: 05.30.Jp, 05.10.Cc

Quantum spins in a bosonic environment are model systems in diverse areas of physics, ranging from dissipative quantum mechanics to impurities in magnets and biological systems [1]. In this Letter we consider the spin-boson model and a generalization thereof to two baths, described by $\mathcal{H}_{\rm sb} = -\vec{h}\cdot\vec{\sigma}/2 + \mathcal{H}_{\rm bath}$, with

$$\mathcal{H}_{\rm bath} = \sum_{i=x,y}\sum_q \left[\omega_q \hat{B}^\dagger_{qi}\hat{B}_{qi} + \lambda_{qi}\frac{\sigma_i}{2}(\hat{B}_{qi} + \hat{B}^\dagger_{qi})\right]. \quad (1)$$

The two-level system (or quantum spin, with $\sigma_{x,y,z}$ being the vector of Pauli matrices) is coupled both to an external field $\vec{h}$ and, via σ_x and σ_y, to two independent bosonic baths, whose spectral densities $J_i(\omega) = \pi\sum_q \lambda^2_{qi}\delta(\omega - \omega_q)$ are assumed to be of power-law form:

$$J_i(\omega) = 2\pi\alpha_i\omega_c^{1-s}\omega^s, \qquad 0 < \omega < \omega_c = 1. \quad (2)$$

Such models are governed by the competition between the local field, which tends to point the spin in the $\vec{h}$ direction, and the dissipative effects of the bosonic baths.

Indeed, the standard one-bath spin-boson model (SBM1), obtained for $\alpha_y = h_y = 0$, exhibits an interesting and much-studied [1–7] quantum phase transition (QPT) from a delocalized to a localized phase, with $\langle\sigma_x\rangle = 0$ or $\neq 0$, respectively, as α_x is increased past a critical coupling $\alpha_{x,c}$. According to statistical-mechanics arguments, this transition is in the same universality class as the thermal phase transition of the one-dimensional (1D) Ising model with $1/r^{1+s}$ interactions. This quantum-to-classical correspondence (QCC) predicts mean-field exponents for $s < 1/2$, where the Ising model is above its upper-critical dimension [8,9].

Checking this prediction numerically turned out to be challenging. Numerical renormalization-group (NRG) studies of SBM1 yielded non-mean-field exponents for $s < 1/2$ [4], thereby seemingly negating the validity of the QCC. However, the authors of Ref. [4] subsequently concluded [10] that those results were not reliable, due to two inherent limitations of the NRG method, which they termed (i) Hilbert-space truncation and (ii) mass flow. Problem (i) causes errors for critical exponents that characterize the flow into the localized phase at zero temperature, since $\langle\sigma_x\rangle \neq 0$ induces shifts in the bosonic displacements $\hat{X}_q = (\hat{B}_q + \hat{B}^\dagger_q)/\sqrt{2}$ of the bath oscillators which diverge in the low-energy limit for $s < 1$ and hence cannot be adequately described in the truncated boson Hilbert space used by the NRG method [11]. Problem (ii) arises for nonzero temperatures, due to the NRG's neglect of low-lying bath modes with energy smaller than temperature [12]. In contrast to the NRG results, two recent numerical studies of SBM1, using Monte Carlo methods [6] or a sparse polynomial basis [5], found mean-field exponents in agreement with the QCC. Nevertheless, other recent works continue to advocate the failure of the QCC [13].

The purpose of this Letter is twofold. First, we show how the problem (i) of Hilbert-space truncation can be controlled systematically by using a variational matrix-product state (VMPS) approach formulated on a Wilson chain. The key idea is to variationally construct an optimized boson basis (OBB) that captures the bosonic shifts induced by $\langle\sigma_x\rangle \neq 0$. The VMPS results confirm the predictions of the QCC for the QPT of SBM1 at $T = 0$. (Problem (ii) is beyond the scope of this work.) Second, we use the VMPS approach to study an XY-symmetric version of the two-bath spin-boson model (SBM2), with $\alpha_x = \alpha_y$. This model arises, e.g., in the contexts of impurities in quantum magnets [14,15] and of noisy qubits [14,16], and displays the phenomenon of "frustration of decoherence" [14]: the two baths compete (rather than cooperate), each tending to localize a different component of the spin. As a result, a nontrivial intermediate-coupling

(i.e., critical) phase has been proposed to emerge for $s < 1$ [15], which has no classical analogue. To date, the existence of this phase could only be established in an expansion in $(1 - s)$, and no numerical results are available. Here we numerically investigate the phase diagram, and, surprisingly, find that the perturbative predictions are valid for a small range of s and α only. We conclusively demonstrate the absence of a QCC for this model.

Wilson chain.—Following Refs. [3,11], which adapted Wilson's NRG to a bosonic bath, we discretize the latter using a logarithmic grid of frequencies $\omega_{ki} \propto \Lambda^{-k}$ (with $\Lambda > 1$ and k a positive integer) and map $\mathcal{H}_{\rm bath}$ onto a so-called Wilson chain of $(L - 1)$ bosonic sites:

$$\mathcal{H}_{\rm bath}^{(L-1)} = \sum_{i=x,y}\Big[\sqrt{\frac{\eta_i}{\pi}}\frac{\sigma_i}{2}(\hat{b}_{1i} + \hat{b}_{1i}^\dagger) + \sum_{k=1}^{L-2} t_{ki}(\hat{b}_{ki}^\dagger \hat{b}_{k+1,i} + \text{H.c.}) + \epsilon_{ki}\hat{n}_{ki}\Big]. \quad (3)$$

Here $\hat{n}_{ki} = \hat{b}_{ki}^\dagger \hat{b}_{ki}$, with eigenvalue n_{ki}, counts the bosons of type i on chain site k; the detailed form of the hopping parameters t_{ki}, on-site energies ϵ_{ki} (both $\propto \Lambda^{-k}$), and the coupling η_i between spin component σ_i and site 1, are obtained following Refs. [17,18]. To render a numerical treatment feasible, the infinite-dimensional bosonic Hilbert space at each site k is truncated by restricting the boson number to $0 \le n_{ki} < d_k$ ($d_k \le 14$ in Refs. [3,11]).

The standard NRG strategy for finding the ground state of $\mathcal{H}_{\rm sb}^{(L)} = -\vec{h}\cdot\vec{\sigma}/2 + \mathcal{H}_{\rm bath}^{(L-1)}$ is to iteratively diagonalize it one site at a time, keeping only the lowest-lying D energy eigenstates at each iteration. This yields an L-site matrix-product state (MPS) [19–21] of the following form (depicted in Fig. 1, dashed boxes):

$$|G\rangle = \sum_{\sigma=\uparrow,\downarrow}\sum_{\{\vec{n}\}} A^0[\sigma]A^1[n_1]\cdots A^{L-1}[n_{L-1}]|\sigma\rangle|\vec{n}\rangle. \quad (4)$$

Here $|\sigma\rangle = |\uparrow\rangle, |\downarrow\rangle$ are eigenstates of σ_x; the states $|\vec{n}\rangle = |n_1, \ldots, n_{L-1}\rangle$ form a basis of boson-number eigenstates within the truncated Fock space, with $\hat{n}_{ki}|\vec{n}\rangle = n_{ki}|\vec{n}\rangle$ and $0 \le n_{ki} < d_k$. For SBM2, $n_k = (n_{kx}, n_{ky})$ labels the states of supersite k representing both chains. Each $A^k[n_k]$ is a matrix (not necessarily square, but of maximal dimension $D \times D$, with A^0 a row matrix and A^{L-1} a column matrix), with matrix elements $(A^k[n_k])_{\alpha\beta}$.

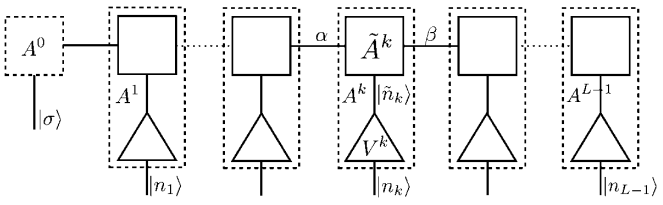

FIG. 1. Depiction of the MPS Eq. (4), with each A-matrix expressed in an optimal boson basis via $A = \tilde{A}V$ [Eq. (5)].

The need for Hilbert-space truncation with small d_k prevents the NRG method from accurately representing the shifts in the displacements $\hat{x}_{ki} = (\hat{b}_{ki} + \hat{b}_{ki}^\dagger)/\sqrt{2}$ that occur in the localized phase. This problem can be avoided, in principle, by using an OBB, chosen such that it optimally represents the quantum fluctuations of *shifted* oscillators, $\hat{x}'_{ki} = \hat{x}_{ki} - \langle\hat{x}_{ki}\rangle$. While attempts to accommodate this strategy within the standard NRG approach were unsuccessful [11], it was shown to work well [5] using an alternative representation of SBM1 using a sparse polynomial basis.

VMPS method.—We now show that an OBB can also be constructed on a Wilson chain. To this end, view the state $|G\rangle$ of Eq. (4) as a MPS ansatz for the ground state of $\mathcal{H}_{\rm sb}^{(L)}$, that is to be optimized *variationally* using standard MPS methods [19–21]. To allow the possibility of large bosonic shifts, we represent the A-matrix elements as [22–24] (Fig. 1, solid lines)

$$(A^k[n_k])_{\alpha\beta} = \sum_{\tilde{n}_k=0}^{d_{\rm opt}-1} (\tilde{A}^k[\tilde{n}_k])_{\alpha\beta} V^k_{\tilde{n}_k n_k} \qquad (k \ge 1). \quad (5)$$

Here V^k in effect implements a transformation to a new boson basis on site k, the OBB, of the form $|\tilde{n}_k\rangle = \sum_{n_k=0}^{d_k-1} V^k_{\tilde{n}_k n_k}|n_k\rangle$ with $0 \le \tilde{n}_k < d_{\rm opt}$. (For SBM2, V^k is a rank-3 tensor.) This ansatz has the advantage that the size of the OBB, $d_{\rm opt}$, can be chosen to be much smaller ($d_{\rm opt} \lesssim 50$) than d_k. Following standard VMPS strategy, we optimize the $\tilde{A}^k$ and V^k matrices one site at a time through a series of variational sweeps through the Wilson chain. As further possible improvement before optimizing a given site, the requisite boson shift can be implemented by hand in the Hamiltonian itself: we first determine the "current" value of the bosonic shift $\langle\hat{x}_{ki}\rangle$ using the current variational state $|G\rangle$, then use it as a starting point to variationally optimize a new $|G'\rangle$ with respect to the shifted Hamiltonian $\mathcal{H}'^{(L)}_{\rm sb}(\hat{b}_{ki}, \hat{b}_{ki}^\dagger) = \mathcal{H}^{(L)}_{\rm sb}(\hat{b}'_{ki}, \hat{b}'^\dagger_{ki})$, with $\hat{b}'_{ki} = \hat{b}_{ki} - \langle\hat{x}_{ki}\rangle/\sqrt{2}$. The shifted OBB protocol, described in detail in Ref. [18], allows shifts that would have required $d_k^{\rm eff} \approx 10^{10}$ states in the original boson basis to be treated using rather small d_k (we used $d_k = 100$).

Spin-boson model.—We applied the VMPS method to SBM1 ($\alpha_y = h_y = 0$), with dissipation strength $\alpha \equiv \alpha_x$ and fixed transverse field $h_z = 0.1$, at $T = 0$. We focussed on the QPT between the delocalized and localized phases in the sub-Ohmic case, $s < 1$. Here, the controversy [4–6,10,13] concerns the order-parameter exponents β and δ, defined via $\langle\sigma_x\rangle \propto (\alpha - \alpha_c)^\beta$ at $h_x = 0$ and $\langle\sigma_x\rangle \propto h_x^{1/\delta}$ at $\alpha = \alpha_c$, respectively. QCC predicts mean-field values $\beta_{\rm MF} = 1/2$, $\delta_{\rm MF} = 3$ for $s < 1/2$ [8], whereas initial NRG results [4] showed s-dependent non-mean-field exponents.

In Fig. 2(a), we show sample VMPS results for $\langle\sigma_x\rangle$ vs $(\alpha - \alpha_c)$ for $s = 0.3$ at $h_x = 0$, where α_c was tuned to yield the best straight line on a log-log plot. The results

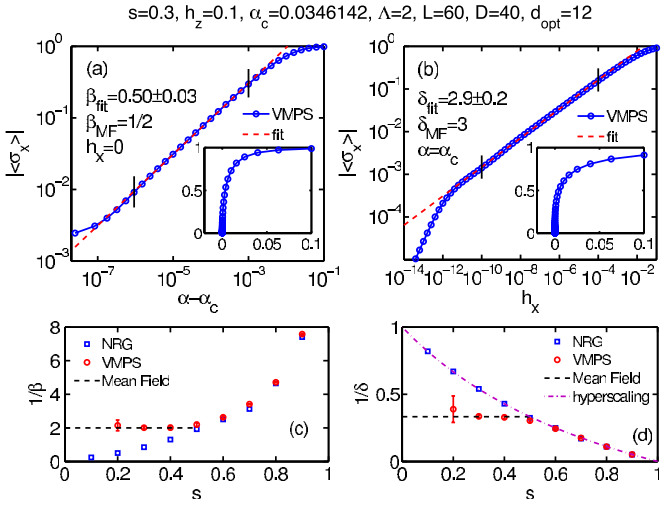

FIG. 2 (color online). VMPS results for the order parameter of SBM1 near criticality. (a) $\langle\sigma_x\rangle$ vs $(\alpha-\alpha_c)$ at $h_x=0$, and (b) $\langle\sigma_x\rangle$ vs h_x at $\alpha=\alpha_c$, on linear plots (insets) or log-log plots (main panels). Dashed lines are power-law fits in the ranges between the vertical marks. (c),(d) Comparison of the exponents β and δ for different s obtained from the VMPS method, NRG studies [4], mean-field theory, and, in (d), the exact hyperscaling result $\delta=(1+s)/(1-s)$ which applies for $s>1/2$. (See also [18], Fig. S7).

display power-law behavior over more than 3 decades, with an exponent $\beta=0.50\pm0.03$. Deviations at small $(\alpha-\alpha_c)$ can be attributed to a combination of finite chain length and numerical errors of the VMPS method. Figure 2(b) shows $\langle\sigma_x\rangle$ vs h_x at $\alpha=\alpha_c$, and a power-law fit over 6 decades results in $\delta=2.9\pm0.2$. Power laws of similar quality can be obtained for all $s\gtrsim0.2$ [18,25] (see [18], Fig. S7).

The exponents β and δ obtained from such fits are summarized in Figs. 2(c) and 2(d). For $s<1/2$ they are consistent with the mean-field values predicted by QCC, also found in Monte Carlo [6] and exact-diagonalization studies [5], but are at variance with the NRG data of Ref. [4]. Since both the NRG and VMPS methods handle the same microscopic model $\mathcal{H}_{\rm sb}^{(L)}$ defined on the Wilson chain, but the VMPS method can deal with much larger $d_k^{\rm eff}$ values ($\lesssim10^{10}$ in Fig. 2) than the NRG method, the incorrect NRG results must originate from Hilbert-space truncation, as anticipated in Ref. [10]. Indeed, artificially restricting d_k to small values in the VMPS approach reproduces the incorrect NRG exponents (see [18], Fig. S6).

Two-bath model.—We now turn to SBM2, a generalization of the spin-boson model. Here, the two baths may represent distinct noise sources [14,16] or XY-symmetric magnetic fluctuations [14,15,26]. Perturbation theory shows that the two baths compete: A straightforward expansion around the free-spin fixed point ($\alpha=h=0$) results in the following one-loop renormalization-group (RG) equations at $\vec{h}=0$:

$$\begin{aligned}\beta(\alpha_x)&=(1-s)\alpha_x-\alpha_x\alpha_y,\\ \beta(\alpha_y)&=(1-s)\alpha_y-\alpha_x\alpha_y.\end{aligned}\tag{6}$$

For $\alpha\equiv\alpha_x=\alpha_y$, these equations predict a stable intermediate-coupling fixed point at $\alpha^*=1-s$, describing a *critical* phase. It is characterized by $\langle\vec{\sigma}\rangle=0$, a *nonlinear* response of $\langle\vec{\sigma}\rangle$ to an applied field $\vec{h}$, and a finite ground-state entropy smaller than ln2, all corresponding to a fluctuating fractional spin [15,27]. This phase is unstable with respect to finite bath asymmetry ($\alpha_x\neq\alpha_y$) and finite field. It had been assumed [15] that this critical phase exists for all $0<s<1$ and is reached for any α.

We have extensively studied SBM2 using the VMPS method; the results are summarized in the $\vec{h}=0$ phase diagram in Fig. 3(a) and the flow diagrams in Fig. 4. Most importantly, we find that the critical phase (CR) indeed exists, but only for $s^*<s<1$, with a universal $s^*=0.75\pm0.01$. Even in this s range, the critical phase is left once α is increased beyond a critical value $\alpha_c(s)$, which marks the location of a continuous QPT into a localized phase (L) with spontaneously broken XY symmetry and finite $\langle\sigma_{x,y}\rangle$. This localized phase exists down to $s=0$, Fig. 3(a). It can be destabilized by applying a transverse field h_z beyond a critical value $h_z^c(\alpha)$, marking the location of a continuous QPT into a delocalized phase (D) with a unique ground state (see Ref. [18], Fig. S9). Finally, for $s\geq1$ we only find weak-coupling behavior; i.e., the impurity behaves as a free (F) spin .

In Fig. 3(b) (and Ref. [18], Fig. S10) we show results for the transverse-field response, $\langle\sigma_z\rangle\propto h_z^{1/\delta'}$, which can be used to characterize the different zero-field phases. $\langle\sigma_z\rangle$ is linear in h_z in L ($\delta'=1$), sublinear in CR ($\delta'>1$), and extrapolates to a finite value in F. For CR, a perturbative calculation gives $1/\delta'=(1-s)+\mathcal{O}([1-s]^2)$ [15] (confirmed numerically in Ref. [18], Fig. S11b), while the

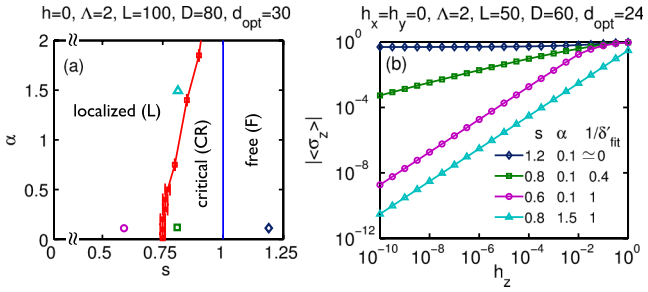

FIG. 3 (color online). (a) Phase diagram of SBM2 in the s-α plane for $\vec{h}=0$, with dissipation strength $\alpha\equiv\alpha_x=\alpha_y$. The critical phase only exists for $s^*<s<1$, and its boundary $\alpha_c\to\infty$ for $s\to1^-$. (Ref. [18] describes the determination of the phase boundary and gives a 3D sketch of the s-α-h_z phase diagram, see Fig. S8.) (b) Tranverse-field response of SBM2, $\langle\sigma_z\rangle\propto h_z^{1/\delta'}$, for four choices of s and α, showing free (diamonds), critical (squares) and localized (triangles, circles) behavior.

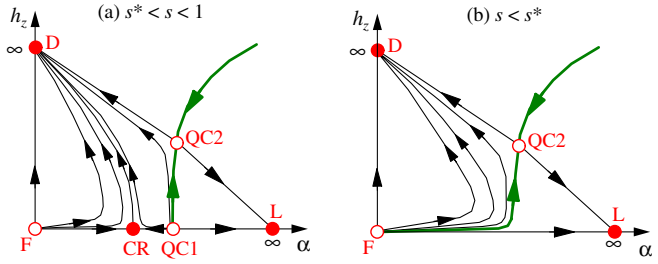

FIG. 4 (color online). Schematic RG flow for SBM2 in the α-h_z plane ($h_x = h_y = 0$). The thick lines correspond to a continuous QPT; the full (open) circles are stable (unstable) fixed points, for labels see text. (a) $s^* < s < 1$: CR is reached for small α and $h_z = 0$, it is separated from L by a QPT controlled by the multicritical QC1 fixed point. Equation (6) implies that CR is located at $\alpha^* = 1 - s + \mathcal{O}[(1-s)^2]$. For finite h_z, a QPT between D and L occurs, controlled by QC2. (b) $0 < s < s^*$: both CR and QC1 have disappeared, such that the only transition is between D and L.

linear response in L corresponds to that of an ordered XY magnet to a field perpendicular to the easy plane.

From the VMPS results, we can schematically construct the RG flow, Fig. 4. There are three stable RG fixed points for $s^* < s < 1$, corresponding to the L, D, and CR phases. From this we deduce the existence of two unstable critical fixed points, QC1 and QC2, controlling the QPTs [Fig. 4(a)]. Equation (6) predicts that, as $s \to 1^-$, CR merges with F; this is consistent with our results for δ' which indicate $\delta' \to \infty$ as $s \to 1^-$ (Ref. [18], Fig. S11b). The behavior of the phase boundary α_c in Fig. 3(a) suggests that QC1 moves towards $\alpha = \infty$ for $s \to 1^-$. Thus, for $s \geq 1$ only F is stable on the $\vec{h} = 0$ axis. Conversely, from Eq. (6) and Fig. 3(a) we extract that, upon lowering s, CR (QC1) moves to larger (smaller) α. From the absence of CR for small s we then conclude that CR and QC1 merge and disappear as $s \to s^{*+}$. Consequently, for $s < s^*$ we have only D and L as stable phases, separated by a transition controlled by QC2, Fig. 4(b). The merger of CR and QC1 at $s = s^*$ also implies that the phase boundary between CR and L in Fig. 3(b) at s^* is vertical at small α (Ref. [18], Sec. V.C), because the merging point on the α axis defines the finite value of α_c at $s \to s^{*+}$.

Taken together, the physics of SBM2 is much richer than that of a classical XY-symmetric spin chain with long-range interactions, which only shows a single thermal phase transition [28]. Given this apparent failure of the QCC for SBM2, it is useful to recall the arguments for QCC for SBM1: A Feynman path-integral representation of Eq. (1), with nonzero h_z, can be written down using eigenstates of both σ_x and σ_z. Integrating out the bath generates a long-range (in time) interaction for σ_x. Subsequently, the σ_z degrees of freedom can be integrated out as well, leaving a model formulated in σ_x only. Reinterpreting the σ_x values for the individual time slices in terms of Ising spins, one arrives at a 1D Ising chain with both short-range and $1/r^{1+s}$ interactions, with the thermodynamic limit corresponding to the $T \to 0$ limit of the quantum model. Repeating this procedure for SBM2 with $\vec{h} = 0$, one obtains a Feynman path integral in terms of eigenstates of σ_x and σ_y. Importantly, both experience long-range interactions and hence neither can be integrated out. This leads to a representation in terms of *two* coupled Ising chains. However, upon reexponentiating the matrix elements, the coupling between the two chains turns out to be imaginary, such that a classical interpretation is *not* possible [29]. In other words, a Feynman path-integral representation of SBM2 leads to negative Boltzmann weights, i.e., a sign problem.

Conclusion.—Our implementation of the OBB-VMPS method on the Wilson chain brings the Hilbert-space truncation problem of the bosonic NRG method under control and allows for efficient ground-state computations of bosonic impurity models. We have used this to verify the QCC in SBM1 and to determine the phase diagram of SBM2, which is shown to violate QCC. This underlines that symmetries are decisive for whether or not a QCC exists. A detailed study of the QPTs of SBM2 is left for future work.

The results for SBM2 also show that the predictions from a weak-coupling RG calculation are *not* valid for all parameters and bath exponents, in contrast to expectations. This implies that studying a *three*-bath version of the spin-boson model, which is related to the physics of a magnetic impurity in a quantum-critical magnet [15,27], is an interesting future subject.

We thank A. Alvermann, S. Florens, S. Kirchner, K. Ingersent, Q. Si, A. Schiller, and T. Vojta for helpful discussions. This research was supported by the Deutsche Forschungsgemeinschaft through SFB/TR12, SFB631, FOR960, by the German-Israeli Foundation through G-1035-36.14, and the NSF through PHY05-51164.

[1] A. J. Leggett *et al.*, Rev. Mod. Phys. **59**, 1 (1987).
[2] S. K. Kehrein and A. Mielke, Phys. Lett. A **219**, 313 (1996).
[3] R. Bulla, N. Tong, and M. Vojta, Phys. Rev. Lett. **91**, 170601 (2003).
[4] M. Vojta, N. Tong, and R. Bulla, Phys. Rev. Lett. **94**, 070604 (2005).
[5] A. Alvermann and H. Fehske, Phys. Rev. Lett. **102**, 150601 (2009).
[6] A. Winter, H. Rieger, M. Vojta, and R. Bulla, Phys. Rev. Lett. **102**, 030601 (2009).
[7] H. Wong and Z. Chen, Phys. Rev. B **77**, 174305 (2008).
[8] M. E. Fisher, S. K. Ma, and B. G. Nickel, Phys. Rev. Lett. **29**, 917 (1972).
[9] E. Luijten and H. W. J. Blöte, Phys. Rev. B **56**, 8945 (1997).

[10] M. Vojta, N. Tong, and R. Bulla, Phys. Rev. Lett. **102**, 249904(E) (2009).
[11] R. Bulla, H. J. Lee, N. H. Tong, and M. Vojta, Phys. Rev. B **71**, 045122 (2005).
[12] M. Vojta, R. Bulla, F. Güttge, and F. Anders, Phys. Rev. B **81**, 075122 (2010).
[13] S. Kirchner, Q. Si, and K. Ingersent, Phys. Rev. Lett. **102**, 166405 (2009).
[14] A. H. Castro Neto, E. Novais, L. Borda, G. Zarand, and I. Affleck, Phys. Rev. Lett. **91**, 096401 (2003); E. Novais, A. H. Castro Neto, L. Borda, I. Affleck, and G. Zarand, Phys. Rev. B **72**, 014417 (2005).
[15] L. Zhu and Q. Si, Phys. Rev. B **66**, 024426 (2002); G. Zarand and E. Demler, Phys. Rev. B **66**, 024427 (2002).
[16] D. V. Khveshchenko, Phys. Rev. B **69**, 153311 (2004).
[17] R. Žitko and T. Pruschke, Phys. Rev. B **79**, 085106 (2009).
[18] See Supplemental Material at http://link.aps.org/supplemental/10.1103/PhysRevLett.108.160401 for a detailed description of our VMPS approach and additional numerical results on SBM1 and SBM2.
[19] A. Weichselbaum, F. Verstraete, U. Schollwöck, J. I. Cirac, and J. von Delft, Phys. Rev. B **80**, 165117 (2009).
[20] H. Saberi, A. Weichselbaum, and J. von Delft, Phys. Rev. B **78**, 035124 (2008).
[21] U. Schollwöck, Ann. Phys. (Leipzig) **326**, 96 (2011).
[22] C. Zhang, E. Jeckelmann, and S. R. White, Phys. Rev. Lett. **80**, 2661 (1998).
[23] A. Weiße, H. Fehske, G. Wellein, and A. R. Bishop, Phys. Rev. B **62**, R747 (2000).
[24] Y. Nishiyama, Eur. Phys. J. B **12**, 547 (1999).
[25] For very small s, high-accuracy numerical calculations inside the localized phase become prohibitively expensive.
[26] S. Kirchner, L. Zhu, Q. Si, and D. Natelson, Proc. Natl. Acad. Sci. U.S.A. **102**, 18 824 (2005).
[27] M. Vojta, C. Buragohain, and S. Sachdev, Phys. Rev. B **61**, 15 152 (2000).
[28] J. M. Kosterlitz, Phys. Rev. Lett. **37**, 1577 (1976).
[29] T. Vojta (private communication).